

# DEVELOPMENT OF A COMPACT X-RAY PIV SYSTEM AND NEW X-RAY FLOW TRACERS

## *Visualization of Opaque Biofluid Flows using X-ray PIV System*

Sang Joon Lee and Sung Yong Jung

*Center for Biofluid and Biomimic Research, Department of Mechanical Engineering, Pohang University of Science and Technology (POSTECH), San 31, Hyojadong, Pohang 790-784, South Korea*

**Keywords:** Medical X-ray, PIV (Particle Image velocimetry), Microparticles, X-ray contrast.

**Abstract:** A compact X-ray particle image velocimetry (PIV) system employing a medical X-ray tube as a light source was developed to obtain quantitative velocity field information of opaque flows. The X-ray PIV system consists of a medical X-ray tube, an X-ray CCD camera, a programmable shutter for generating a pulse-type X-ray beam, and a synchronization device. Through performance tests, the feasibility of the developed X-ray PIV system as a flow measuring device was verified. In applying the developed system to biofluid flows, the most important prerequisite is to develop suitable flow tracers which should be detected clearly by the X-ray imaging system. Iopamidol was encapsulated into the poly(vinyl alcohol) (PVA) microparticles to fabricate such flow tracers. The characteristics of the fabricated microparticles were checked. With increasing the amount of crosslinker, the degree of crosslinking and the efficiency of the Iopamidol encapsulation were increased. This compact X-ray PIV system is a unique and useful for investigating various biofluid flows in laboratory experiments.

## 1 INTRODUCTION

Recently, abnormal blood flows such as formation of recirculation flow or low wall shear stress have been known to play a key role in the pathology of atherosclerosis (Malek et al., 1999). For more detailed and meaningful elucidation about these hemodynamic phenomena related with vascular diseases, it is definitely needed to get quantitative hemodynamic information of blood flows related with the vascular diseases with high spatial resolution of tens micrometer and temporal resolution in the order of millisecond.

Currently, various medical instruments such as Doppler ultrasonography, MRI (Magnetic Resonance Imaging) and X-ray angiography have been used to measure the blood flow. However, each method has intrinsic problems in diagnosing the hemodynamic aspects of vascular diseases in more detail. Doppler ultrasonography is one dimensional point measurement tool and has relatively high errors caused by its angle dependency. For the case of MRI method, real time measuring is very limited due to low temporal resolution and its spatial resolution is not so good enough. X-ray angiography

provides morphological information of blood vessels and blood velocity can be evaluated using concentration difference of iodine contrast media from consecutive digital images (Rhode et al., 2005). Unfortunately, this method is also not suitable for acquiring blood flow information inside blood vessels due to low spatial resolution and it is also limited to apply to flow in a short vessel. These limitations of conventional clinical diagnosis methods bring about a strong demand on a more effective and advanced analysis tool which can provide more detailed, quantitative hemodynamic information of blood flows.

On the other hand, The particle image velocimetry (PIV) method, which extracts velocity vectors of tracer particles seeded in a flow by obtaining their displacement, has been accepted as one of the reliable velocity measurement techniques with high spatial and temporal resolutions (Adrian, 1991). However, it is difficult for the PIV method to visualize the blood flows inside blood vessels of vascular diseases under in vivo condition, because the conventional PIV techniques have used a visible light source which cannot transmit an opaque blood. To overcome these limitations on conventional PIV

systems, a transmission-type light source such as X-ray or ultrasonic wave should be used instead of visible light.

An X-ray PIV technique using a synchrotron X-ray source was developed (Lee and Kim, 2003). Thereafter, several application studies have been performed, such as blood flows (Kim and Lee, 2006), flow of micro bubbles (Lee and Kim, 2005), glycerin flow (Im et al. 2007), sap flow in a bamboo leaf (Lee and Kim, 2008), and 3D X-ray PIV application (Fouras, 2008). The synchrotron X-ray PIV system, however, is not easy to use for general-purpose research works because synchrotron facility is very limited to getting beam times and synchrotron X-rays are usually dangerous for biological samples due to its high flux. Therefore, in the consideration of X-ray PIV applications, the substitution of the synchrotron X-ray source with a medical X-ray tube is a straightforward and natural consequence.

As far as we surveyed, there has been no trial conducted to combine the medical X-ray imaging method and the PIV velocity field measurement technique with seeding fine tracer particles in the flow. In this study, we established a new compact X-ray PIV system employing a conventional medical X-ray tube, an X-ray CCD camera equipped with the frame-straddling feature, and a newly developed mechanical shutter for generating double pulses of X-rays. This compact X-ray PIV system has a spatial resolution of tens of micrometers and a temporal resolution of several milliseconds.

In applying the developed system to blood flows, the most important prerequisite is to develop suitable flow tracers which should be detected clearly by the X-ray imaging system. The tracers should be able to follow properly the fluid flow to be measured. In addition, they should be bio-compatible and can be removed safely without any harm to the living organism. In earlier X-ray PIV experiments, alumina particles (Lee and Kim, 2003) and silver-coated hollow glass beads (Fouras et al., 2007; Im et al., 2007) were used to track the fluid flows. However none of them is suitable for visualizing blood flows, because their specific weight is relatively high and they are not bio-compatible nor bio-degradable. The speckle pattern of red blood cells was also used to get their velocity information (Kim and Lee, 2006). However, this method is not conducive to in-vivo applications due to image blurring and noises generated by the surrounding materials such as tissues. Therefore, the in-vivo velocity field measurements of opaque biofluid flows have not been fully satisfactory so far.

Poly(vinyl alcohol) (PVA) is a carbon-backed polymer that is biodegradable under both aerobic (Nord, 1936) and anaerobic (Matsumura et al., 1993) conditions. In this point of view, the grafting functional oligomers were incorporated into PVA chain. The PVA chain has been tried to be modified widely where the biodegradable vinyl alcohol block plays an essential role in the functional polymer composites (Matsumura et al., 1988). Iopamidol (also known as Solustrast®) is a nonionic, low-osmolar iodinated contrast agent developed by Bracco. It has been commonly used in clinical angiography to enhance the absorption contrast. In this study, Iopamidol was encapsulated into bio-compatible and bio-degradable PVA microparticles. The Iopamidol encapsulated PVA was templated by W/O (water-in-oil) emulsion. It was specially designed as flow tracers for quantitative X-ray imaging of biofluid flows. The compact X-ray PIV system and new X-ray flow tracers are expected to expand the application areas of the X-ray PIV technique even to the in vivo velocity field measurement of various blood flows.

## 2 COMPACT MEDICAL X-RAY PIV SYSTEM

Figure 1 shows the schematic diagram of the compact X-ray PIV system developed in this study. In the compact X-ray PIV system, a conventional medical X-ray tube was used as a light source. The most important issue in PIV measurements is acquiring two consecutive flow images within a short time interval. For this, double pulses of X-rays should be generated from an X-ray tube and then a detector needs to record two consecutive X-ray

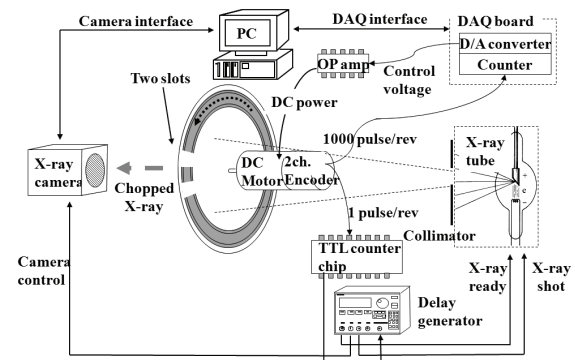


Figure 1: Schematic diagram of the established compact X-ray PIV system.

images with high spatial resolution and good sensitivity.

The pixel size of most clinical X-ray detectors used in medical radiography is larger than 50  $\mu\text{m}$ . In addition, the conventional X-ray detectors cannot provide the frame-straddling feature indispensable for PIV measurements. In this study, we purchased a customized X-ray CCD camera of  $4000 \times 2672$  pixels from Hamamatsu Co. The architecture of this CCD camera is identical with that of a cooled CCD camera, the exception is that a CsI scintillation crystal of 100 $\mu\text{m}$  in thickness is adhered to the top of the CCD sensor array. Due to high sensitivity of the CsI scintillator, this X-ray CCD is well fitted to the compact X-ray PIV system for acquiring X-ray images suitable for PIV velocity field measurement.

Related to the medical X-ray source, because an X-ray tube with a smaller focal spot size can provide clearer particle images (Jenneson et al., 2003), we employed an X-ray tube (Varian A272) with a focal spot size of 0.3/0.6mm at 100/300 mA for 40~150 kVp. The maximum exposure time of the X-ray tube (Varian A272) is 5sec at 200mA and 60kVp. The total pulse length of X-ray beam fired from the X-ray tube is an input parameter on the X-ray tube controller (SMS-525). In this experiment, the total pulse length was fixed at 100 ms. This long pulse was chopped into two short X-ray pulses by using a mechanical shutter newly developed in this study. The actual pulse length of each short pulse was 5 ms and the time interval between two X-ray pulses was 20 ms. This X-ray tube was synchronized through an external triggering switch by using a photocoupler chip and a transistor transistor logic (TTL) signal from a delay generator.

The X-ray shutter system connected with a 4-channel synchronizer plays a key role in synchronizing the X-ray tube, the X-ray detector, and the rotating disc of the shutter. The delay generator takes the pulse signal of 1 pulse/rev from the encoder of the DC motor and then the X-ray tube takes two pulse signals of "X-ray ready" and "X-ray shot" from the delay generator. The X-ray CCD camera is synchronized by using the delay generator. The timing sequence for synchronization of the compact X-ray PIV system is mainly determined from the disk geometry and motor rotation speed. Finally, the X-ray PIV system can provide two chopped X-ray pulses for recording two consecutive X-ray images.

### 3 PERFORMANCE EVALUATION

To check the feasibility of the developed compact X-ray PIV system, we measured velocity fields of a flow of glycerin ( $\rho = 1.260 \text{ g/cm}^3$ ) inside an opaque tube of 4 mm in diameter. The width of an X-ray pulse fired from the X-ray tube was 100 ms. This pulse was chopped into two short X-ray pulses of 5 ms width with a time interval of 20 ms using the developed X-ray shutter. The X-ray CCD camera then recorded two X-ray images consecutively.

Tungsten oxide particles were used as tracer particles. The particle has a relatively high density ( $\rho_p$ ) of 7.2  $\text{g/cm}^3$  and a high attenuation coefficient for X-rays. Since the size of the tracer particles is in the range of 10~50  $\mu\text{m}$  in diameter, it is appropriate for recording images with the X-ray CCD camera. Glycerin solution having a viscosity coefficient ( $\mu_f$ ) of 1.50  $\text{N}\cdot\text{s/m}^2$  was used as a working fluid. The free-falling speed of the tracer particles ( $U_g$ ) in the glycerin fluid is in the range of 0.216~5.395  $\mu\text{m/s}$ , a negligibly small under the given experimental condition. We tested a tube flow at two different mean velocities of 1mm/s and 2mm/s. As the two velocity fields obtained were substantially the same, the experimental result measured at the mean velocity of 2mm/s is only represented in this paper.

The size of interrogation area was  $16^{(H)} \times 128^{(V)}$

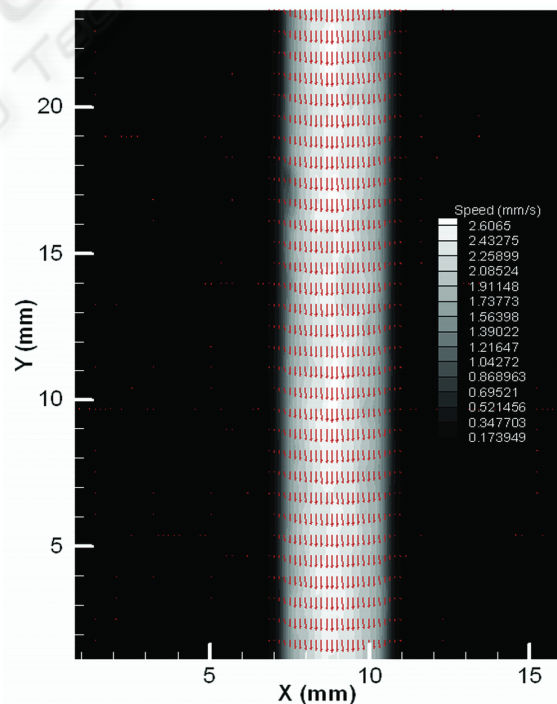


Figure 2: Mean velocity field of glycerin flow in a tube measured by the compact X-ray PIV system.

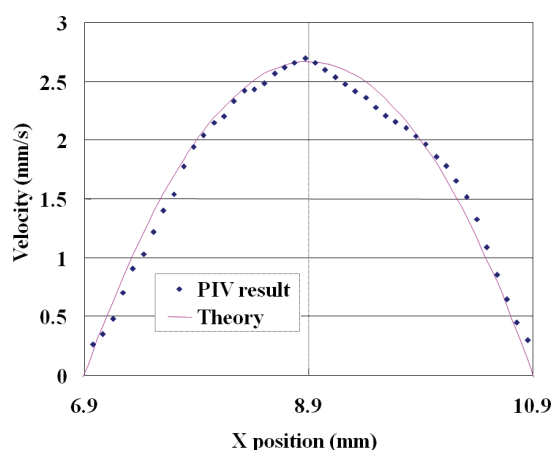


Figure 3: Comparison of velocity profiles of the test flow in a tube.

pixels in the consideration of dominant longitudinal flow. The number of particles in each interrogation window was about 4-8 on average. We obtained 25 pairs of X-ray images to get velocity field information.

The images of tracer particles seeded into the opaque tube are apparent. In addition, there is no optical distortion in the region near the tube wall. From the two consecutive X-ray images, quantitative velocity field information was obtained by applying a cross-correlation PIV algorithm. Figure 2 represents a typical mean velocity field obtained by ensemble averaging 25 instantaneous velocity fields. The glycerin flow in the circular tube seems to have a parabolic velocity profile with a maximum value at the tube center. Actually, it is nearly impossible for other flow measurement techniques to obtain this kind of quantitative velocity field information of a flow inside an opaque conduit.

Figure 3 shows the velocity profile across the tube diameter, extracted from the mean velocity field. The solid dots are the experimental data obtained and the parabolic line represents the theoretical velocity profile. The experimental results measured with the developed compact X-ray PIV system agree well with the theoretical one. The spatial resolution between two adjacent velocity vectors is about 91  $\mu\text{m}$ , which is much better than that of the MRI method (Pahernik et al. 2001). The small discrepancy between the two velocity profiles seems to be attributed to the density difference of the tracer particles and the working fluid. In addition, the cohesion feature of tungsten particles in glycerin also has some influence on the velocity difference.

#### 4 FABRICATION OF NEW X-RAY FLOW TRACERS

In applying the compact X-ray PIV system to blood flows, new microparticles were developed as suitable flow tracers. The detailed flow chart of particle synthesis procedure is schematically shown in Fig. 4. 3 ml of oil soluble Span 80 (HLB=4.3) was dissolved in 100 ml n-hexane (A). 41 wt% Iopamidol stock solution and 16 wt% of PVA aqueous solution were prepared overnight at the room temperature and 70°C, respectively. 3 ml of PVA aqueous solution ( $4.8 \times 10^{-2}$  g/mL) and 7 ml of Iopamidol stock solutions ( $4.8 \times 10^{-1}$  g/mL) were mixed (B). The oil phase (A) was added in drop forms to the water phase (B) by stirring at 4400 rpm. After stirring for one hour at the room temperature, emulsion picture was taken using an optical microscopy to check the size of the microreactor. Controlled amount of glutaraldehyde (GA) was introduced as a crosslinker with proper amount of hydrochloric acid (0.04 ~ 0.16g) for activation. The homogenizing process was performed for additional 6 hours at the room temperature with keeping the same stirring rate. The emulsion formation (4400 rpm) was followed by the overnight stabilization. To remove unreacted residues, the filtering and washing process were repeated several times with n-hexane and de-ionized (DI) water and then centrifuged to get the settle-downed particles. The filtered particles were de-moisturized in the drying oven at 60°C and then placed in the desiccator until there is no further variation in their mass.

The microdroplets of the fabricated water-in-oil (W/O) emulsion in this study were several micrometers in diameter and their size distribution was relatively narrow. After the formation of stable emulsion, the designed amount of crosslinker was

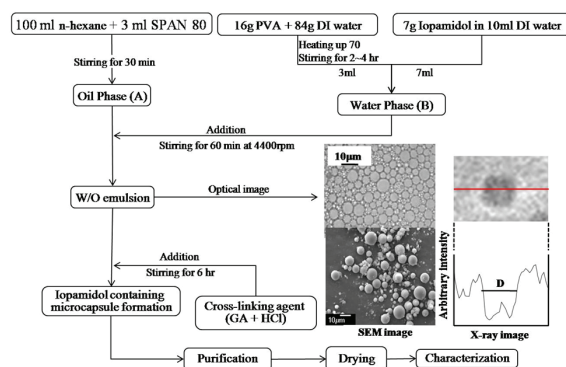


Figure 4: Schematic diagram of the microparticle synthesis.

Table 1: Specifications of the particles fabricated in this study.

Particle	Crosslinker ratio (a)	Average diameter [ $\mu\text{m}$ ]	Degree of swelling [%]	Degree of crosslinking [%]	Amount of Iopamidol	
					EDS [atomic %]	$^1\text{H}$ NMR [mole]
#1	2.5	6.14	250	77	1.52	2.5
#2	5	6.92	183	93	4.83	49.0
#3	10	8.64	125	93	4.04	34.5
Empty capsule	1	9.17	133	74	0	0

incorporated. Four hydroxyl groups of the PVA are supposed to be connected by one glutaraldehyde molecule. Considering the amount of hydroxyl groups in the PVA, three different types of particle sensors were fabricated by changing the amount of glutaraldehyde (GA). For the case of particle #1, 0.00625 mole of GA was incorporated, which corresponds to 2.5 times of the possible crosslinker units in PVA. Likewise, 5 times (0.0125 mole) of GA were added into the particle #2. For the particle #3, 10 times of those (0.025 mole) were added, corresponding to 0.1 mole of hydroxyl groups in the PVA. Table 1 summarizes the specifications of each particle fabricated in this study.

## 5 THE CHARACTERISTICS OF TRACER PARTICLES

The particle size and their distributions were counted and averaged from several images produced through scanning electron microscopy (SEM). The average diameter of the particles ranged from 6 to 9  $\mu\text{m}$ , and this value increased with the increase of the crosslinker (GA) ratio from particles #1 to #3. Therefore, the added crosslinker used in this study contributed to the increased size rather than led to the network shrinkage. The degree of crosslinking was determined by the  $^1\text{H}$  NMR. The chemical shift of particles #1, #2, and #3 were compared with pure Iopamidol, empty capsule, and uncrosslinked PVA. The methylene group newly formed by crosslinking increased along with an increase in crosslinker ratio from particles #1 to #3, while the peaks in the methylene groups in uncrosslinked PVA decreased by that order. As summarized in Table 1, the quantitative degree of crosslinking exhibited a value of 77% in particle #1 and then reached the optimum of 93% in particle #2; no further increase in particle #3 was observed.

Meanwhile, the degree of swelling was measured by dissolving the particles in deionized water until there was no further increase in their mass according to the relation,  $W = (W_s - W_d)/W_d \times 100$  [%], where  $W_s$  is the mass of the fully swollen particle, and  $W_d$  is that of the dried particle. As the added crosslinker increased, the degree of swelling in DI water was observed to show a decreasing trend. The degree of maximum swelling reflects the equilibrium between the dilution of the polymer chain into the solvent and the retractive force produced by the crosslinked junction points that serve to restrict further swelling. Given that the chemical compositions of all the particles are supposed to be similar (similar Flory-Huggins interaction parameter,  $\chi$ ), the difference in the degree of swelling seemed to be mainly caused by the network structure. The particles became less elastic from particles #1 to #3, reflecting more densely crosslinked network structure by that order. The amount of the encapsulated Iopamidol was obtained by measuring the energy dispersive X-ray spectroscopy (EDS) connected with SEM and then averaging the value from the three randomly

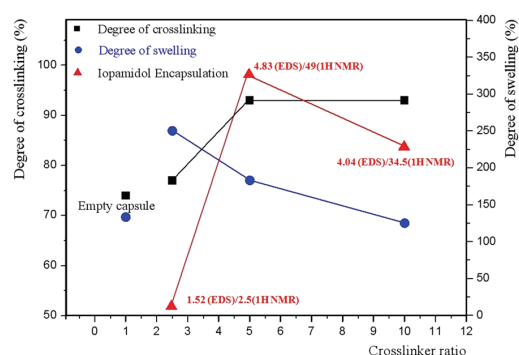


Figure 5: Degree of crosslinking vs. swelling and Iopamidol encapsulation according to the crosslinker ratio.

selected particles. Iopamidol encapsulation was also determined by  $^1\text{H}$  NMR where the chemical shift of

particles #1, #2, and #3 were compared with those of the characteristic methyl group peaks in the pure Iopamidol. In both methods, the efficiency of the Iopamidol encapsulation increased dramatically in particle #2 compared with particle #1 brought about by the increase in the added crosslinker. The amount of Iopamidol reached the maximum in particle #2 and decreased slightly in particle #3. Although the degree of crosslinking detected by the  $^1\text{H}$  NMR was almost same in particles #2 and #3, the degree of swelling in particle #2 was slightly higher. From this, we can assume that particle #2 has a more flexible 3-dimensional structure compared to particle #3, which could lead to higher encapsulation of Iopamidol in the former. The relation between the degrees of crosslinking and swelling, as well as the amount of Iopamidol encapsulations are graphically summarized in Figure 5. Due to the presence of the elastic force equilibrium between the retractive and extended forces, the degrees of crosslinking and the swelling exhibited opposite tendencies, while Iopamidol reached the maximum amount at the optimized encapsulation in particle #2.

## 6 CONCLUSIONS

The compact X-ray PIV system combining the conventional X-ray radiography technique and PIV velocity field measurement method was developed. Through preliminary tests, the spatial and temporal resolution of this system was found to be higher than any conventional clinical instruments. In addition, new X-ray flow tracers were fabricated by encapsulating Iopamidol into bio-compatible polymer PVA. The functional characteristics of the fabricated microparticles were checked. With increasing the amount of crosslinker, the degree of crosslinking and the efficiency of the Iopamidol encapsulation were increased. In near future, the developed system would be employed usefully for measuring *in vivo* velocity field information of blood flows.

## ACKNOWLEDGEMENTS

This work was supported by the Creative Research Initiatives (Diagnosis of Biofluid Flow Phenomena and Biomimic Research) of MEST/KOSEF.

## REFERENCES

- Adrian, R. J. (1991) "Particle-imaging techniques for experimental fluid mechanics", *Annual Review of Fluid Mechanics*, Vol. 23, pp. 261-304.
- Fouras, A., Dusting, J., Lewis, R. and Hourigan, K. (2007) "Three-dimensional synchrotron X-ray particle image velocimetry", *Journal of Applied Physics*, Vol. 102, 064916.
- Im, K.S., Fezzaa, K., Wang, Y. J., Liu, X., Wang, J. and Lai, M. C. (2007) "Particle tracking velocimetry using fast X-ray phase-contrast imaging", *Applied Physics Letters*, Vol. 90, 091919.
- Jenneson, P. M., Gilboy, W. B., Morton, E. J. and Gregory, P. J. (2003) "An-ray micro-tomography system optimised for the low-dose study of living organisms", *Applied radiation and isotopes*, Vol. 58, pp. 177-181.
- Kim, G. B. and Lee, S. J. (2006) "X-ray PIV measurements of blood flows without tracer particles", *Experiments in Fluids*, Vol. 41, pp. 195-200.
- Lee, S. J. and Kim, G. B. (2003) "X-ray Particle Image Velocimetry for measuring quantitative flow information inside opaque objects", *Journal of Applied Physics*, Vol. 94, pp. 3620-3623.
- Lee, S. J. and Kim, S. (2005) "Simultaneous measurement of size and velocity of microbubbles moving in an opaque tube using an X-ray particle tracking velocimetry technique", *Experiments in Fluids*, Vol. 39, pp. 492-497.
- Lee, S. J. and Kim, Y. M. (2008) "In vivo Visualization of the Water-refilling Process in Xylem Vessels Using X-ray Micro-imaging", *Annals of Botany*, Vol. 101, pp. 595-602.
- Malek, A., Alper, S. and Izumo, S. (1999) "Hemodynamic shear stress and its role in atherosclerosis", *JAMA*, Vol. 282, pp. 2035-2042.
- Matsumura, S., Kurita, H. and Shimokobe, H. (1993) "Anaerobic biodegradability of polyvinyl alcohol", *Biotechnology Letters*, Vol. 15, pp. 749-754.
- Matsumura, S., Takahashi, J., Maeda, S. and Yoshikawa, S. (1988) "Molecular design of biodegradable functional polymers, 1. Poly(sodium vinylacetate)", *Die Makromolekulare Chemie, Rapid Communications*, Vol. 9, pp. 1-5.
- Nord, F. F. (1936) "Dehydrogenation activity of Fusarium lini B", *Naturwissenschaften*, Vol. 24, 763.
- Pahernik, S., Griebel, J., Botzlar, A., Gneiting, T., Brandl, M., Dellian, M. and Goetz, A.E. (2001) "Quantitative imaging of tumour blood flow by contrast-enhanced magnetic resonance imaging", *British Journal of Cancer*, Vol. 85, pp. 1655-1663.
- Rhode K.S., Lambrou T., Hawkes D.J. and Seifalian A.M. (2005) "Novel approaches to the measurement of arterial blood flow from dynamic digital x-ray images", *IEEE TRANSACTIONS ON MEDICAL IMAGING*, Vol. 24, pp. 500-513.